

# Study of optimization of images in interventional fluoroscopy\*

*Estudo de otimização de imagens em fluoroscopia intervencionista*

Alexandre Parizoti<sup>1</sup>, Thomaz Ghilardi Netto<sup>2</sup>

**Abstract** **OBJECTIVE:** The objective of the present study is to analyze the optimization of fluoroscopic image quality and patient entrance surface air kerma rate in interventional radiology procedures, utilizing a phantom adapted for fluoroscopy. **MATERIALS AND METHODS:** The authors utilized a phantom developed for evaluating conventional radiological images adapted for fluoroscopy through the addition of two catheters with different diameters, both of them utilized in interventional radiology. The patient entrance surface air kerma rate was determined with the aid of this phantom. **RESULTS:** The evaluation of technical parameters for different exposure modes of a digital fluoroscopic imaging system has allowed the determination of the air kerma rate, enabling the optimization of the image quality in interventional procedures. The decrease in the patient entrance surface air kerma rate may achieve 67%. **CONCLUSION:** The optimization of fluoroscopic image quality achieved with a phantom allows reducing the patient entrance surface air kerma with no significant loss of diagnostic performance.

*Keywords:* Images optimization; Fluoroscopy; Phantom; Dose reduction.

**Resumo** **OBJETIVO:** O objetivo deste trabalho é o de estudar a otimização da qualidade da imagem fluoroscópica e a taxa de kerma no ar de entrada na superfície do paciente em procedimentos de radiologia intervencionista, utilizando-se de um objeto simulador adaptado para fluoroscopia. **MATERIAIS E MÉTODOS:** Foi utilizado um objeto simulador desenvolvido para avaliação de imagens em radiologia convencional. O objeto simulador foi adaptado para fluoroscopia mediante incorporação de dois cateteres com diferentes espessuras, ambos utilizados em radiologia intervencionista. Os níveis de taxa de kerma no ar de entrada na superfície do paciente foram determinados utilizando-se este objeto simulador. **RESULTADOS:** A avaliação dos parâmetros técnicos para diversos modos de exposição de um equipamento fluoroscópico com digitalização de imagens permitiu estabelecer os indicadores de taxa de kerma no ar, que permitem a otimização da qualidade das imagens em procedimentos intervencionistas. A redução na taxa de kerma no ar de entrada na superfície do paciente pode chegar a 67%. **CONCLUSÃO:** A otimização da qualidade da imagem utilizando-se um objeto simulador possibilita reduzir a taxa de kerma no ar de entrada na superfície do paciente, sem perda considerável de informação diagnóstica.

*Unitermos:* Otimização de imagens; Fluoroscopia; Objeto simulador; Redução de dose.

Parizoti A, Ghilardi Netto T. Study of optimization of images in interventional fluoroscopy. *Radiol Bras.* 2009;42(6):375-378.

## INTRODUCTION

The production of fluoroscopic images, particularly the interventional ones, is

among radiologic procedures involving the highest radiation exposure for both patients and medical professionals involved. According to the ALARA principle<sup>(1)</sup>, it is extremely important to implement programs of quality assurance and radioprotection<sup>(2,3)</sup> with the objective of optimizing the imaging quality and that the radiation exposure rates are brought down as low as feasible. Therefore, it is essential to evaluate the parameters involved in the optimized production of radiographic images<sup>(4,5)</sup> with the aid of phantoms.

Thus, the main objective of the present study was to evaluate fluoroscopic images, as well as the effect of the variation in the entrance surface air kerma rate for differ-

ent exposure modes, by utilizing a phantom adapted for interventional procedures<sup>(6)</sup>.

## MATERIALS AND METHODS

The experimental procedure was performed with a BV Pulsera C-arm type fluoroscopic system (Philips Medical Systems; Eindhoven, The Netherlands), with images digitization. The phantom utilized in the present study was adapted for fluoroscopy, consisting of a patient simulator and a realistic-analytic phantom<sup>(7)</sup>, as shown on Figure 1, simulating human anatomy structures<sup>(8)</sup>, relevant for radiological procedures. The adaptation of the realistic-analytic phantom consisted of the implantation

\* Study developed at Department of Physics and Mathematics, Faculdade de Filosofia Ciências e Letras de Ribeirão Preto da Universidade de São Paulo (FFCLRP-USP), Ribeirão Preto, SP, Brazil.

1. Medical Physicist, Master in Physics Applied to Medicine and Biology, Department of Physics and Mathematics - Faculdade de Filosofia Ciências e Letras de Ribeirão Preto da Universidade de São Paulo (DFM/FFCLRP-USP), Ribeirão Preto, SP, Brazil.

2. Titular Professor, Coordinator for the Unit of Medical Physics at Hospital das Clínicas da Faculdade de Medicina de Ribeirão Preto da Universidade de São Paulo (HCFMRP-USP), Ribeirão Preto, SP, Brazil.

Mailing address: Dr. Alexandre Parizoti. Rua Eliza dos Reis Lourenço, 175, Parque Primavera. São Joaquim da Barra, SP, Brazil, 14025-670. E-mail: parizoti@yahoo.com.br

Received April 20, 2009. Accepted after revision August 27, 2009.

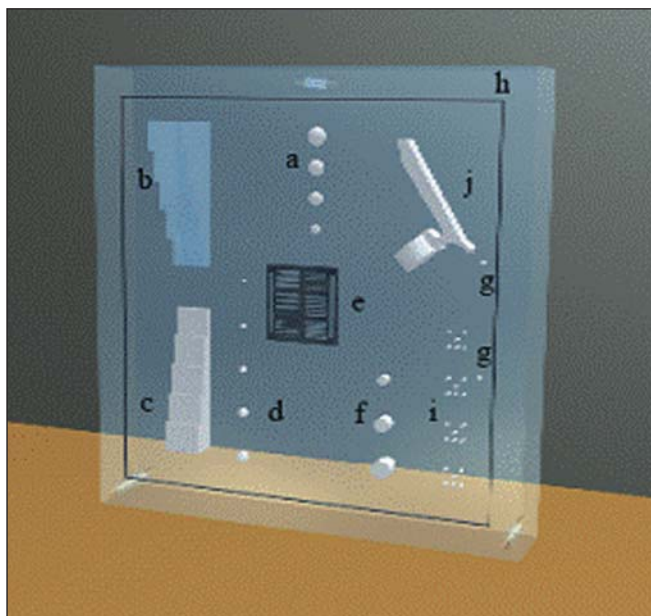


**Figure 1.** Geometrical distribution of the realistic-analytic phantom components.



**Figure 2.** Realistic-analytic phantom adapted for fluoroscopy.

of two catheters utilized in pelvic and cerebral vascular interventions, respectively with 1.65 mm and 0.8 mm thicknesses, as shown on Figure 2. The air kerma rates were determined by a 10x5-60 ionization chamber (Radcal Corp.; Monrovia, USA) coupled with an electrometer 9015 model (Radcal Corp.; Monrovia, USA).

The measurements of entrance surface air kerma rates were performed with 38 mm-thick aluminum plates, likewise in procedures of constancy tests<sup>(9)</sup>, besides the phantom simulating the patient. In both cases, the same geometric configuration adopted for the performance typical studies was utilized with a 100 cm-distance between the x-ray tube and the image intensifier, and the ionization chamber positioned at a 30 cm-distance from the image intensifier input, and the test body at a 20 cm-distance from the ionization chamber, that is to say in the middle point between the focal point and the image intensifier<sup>(9)</sup>.

The evaluation of image quality was performed with the realistic-analytic phantom duly adapted for fluoroscopy with the two catheters implantation. Such images evaluation was performed with the assistance of medical radiologists and was focused on the conditions of visualization of

each structure. The phantom adapted for fluoroscopy was utilized in the acquisition of about a hundred fluoroscopic images covering the full range of exposure modes available in the system as follows: three low-definition fluoroscopy (LDF) and six high-definition fluoroscopy (HDF).

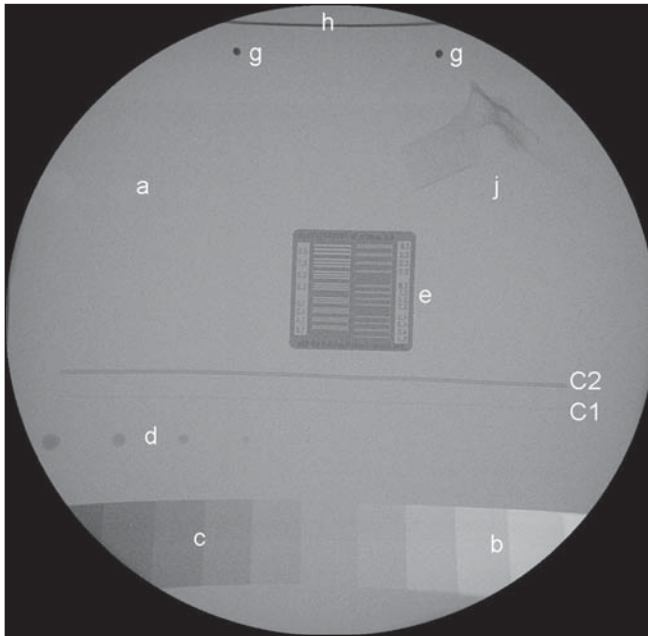
## RESULTS

Figure 3 presents a picture of the phantom adapted for fluoroscopy, as well as the structures of interest for the interventional procedure that allowed the visualization of images besides the catheters C1 and C2: (a) the nylon caps simulating tumors; (b) the air-acrylic wedge-shaped phantom simulating the body cavities; (c) the acrylic-PVC wedge shaped simulating bone structures; (d) aluminum spheres representing the bone tissue borders; (e) the device for evaluating resolution in line pairs/mm; (g) iron spheres for analyzing magnification; (h) tin wire for field evaluation; (j) half thoracic vertebra. Thus, one can evaluate thickness differences of a specific material or materials of very close effective atomic numbers, as well as visualizing and establishing bone structures limits, visualizing and guiding extremely thin catheters utilized in cerebral interventional procedures,

and estimating limits for the system spatial resolution.

The images of the phantom adapted for fluoroscopy obtained on different exposure modes demonstrate that there is no significant loss of diagnostic information for the different exposure modes as shown on Figure 4. In other words, in most of cases, the variation in the exposure conditions which reduces the dose to the patient does not affect the fluoroscopic image, neither condemn nor impede the interventional procedure. This fact is evidenced by the observation of Figure 4 in correlation with Table 1, where the image A was obtained with a mean air kerma rate of  $4.6 \pm 0.1$  mGy/minute, while the image C was obtained with a mean air kerma rate of  $1.58 \pm 0.01$  mGy/minute. In this case, the reduction in the mean air kerma rate achieves 67%.

In spite of the dynamic nature of images in interventional fluoroscopy, the present study was developed with a static phantom. Therefore, it is possible that in some cases the utilization of techniques to reduce the air kerma rate is not feasible. Resources provided by the fluoroscopic equipment, should be utilized as possible, since they play a relevant role in the optimization of images quality and, consequently, in the reduction of the dose to the patient.



**Figure 3.** Radiographic image of the realistic-analytic phantom adapted for fluoroscopy.

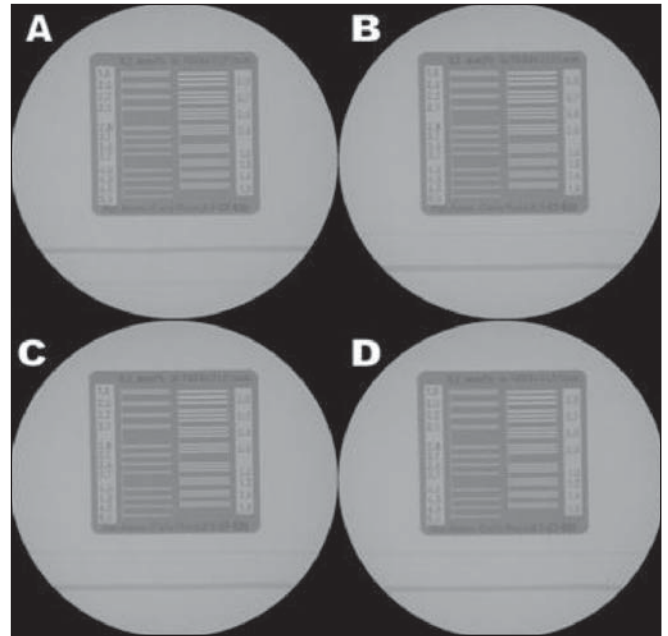


**Figure 4.** Effect of the variation in the air kerma rate on image A – continuous mode; B – half dose; C – quarter dose; D – pulsed (8 frames/s).

Table 1 presents the entrance surface air kerma rate obtained with the phantom for the different exposure modes, demonstrating the alternatives for reduction of the dose to the patient during the examination. The abbreviations LDF and HDF correspond to the low- and high-definition fluoroscopic exposure modes, respectively.

Table 2 presents the measurements of the typical entrance surface air kerma rates obtained with aluminum plates as suggested by the constancy test protocols, so one can compare the values on Tables 1 and 2, demonstrating the equivalence between the phantom adapted for fluoroscopy and the 38 mm-thick aluminum plates in terms of entrance surface air kerma rates.

**DISCUSSION**

Figure 3 shows the image of the phantom adapted for evaluating fluoroscopy equipment. The images obtained at different exposure modes did not demonstrate any significant loss of diagnostic information, highlighting that the exposure modes with low frame rate pulsed fluoroscopy and the continuous mode of quarter dose fluoroscopy constitute the options with lowest exposure to the patients.

The values obtained for entrance surface air kerma rate with the phantom in-

**Table 1** Phantom entrance surface air kerma rate.

	Exposure mode	Voltage (kVp)	Amperage (mA)	Mean air kerma rate (mGy/min)	
LDF	Continuous	68	2.4	4.6 ± 0.1	
	1/2 dose	69	1.3	3.07 ± 0.01	
	1/4 dose	69	0.7	1.58 ± 0.01	
HDF	Continuous	68	5.8	10.9 ± 0.1	
	1/2 dose	69	3.1	6.73 ± 0.01	
	1/4 dose	70	1.6	3.68 ± 0.02	
	Pulsed	3 frames/s	70	1.8	4.16 ± 0.07
		5 frames/s	70	3.0	6.93 ± 0.01
8 frames/s		70	4.4	10.18 ± 0.01	

**Table 2** Patient entrance surface air kerma rate.

	Exposure mode	Voltage (kVp)	Amperage (mA)	Mean air kerma (mGy/min)	
LDF	Continuous	68	2.4	3.37 ± 0.03	
	1/2 dose	69	1.3	2.88 ± 0.01	
	1/4 dose	69	0.7	1.50 ± 0.01	
HDF	Continuous	68	5.7	10.63 ± 0.09	
	1/2 dose	69	3.0	6.37 ± 0.06	
	1/4 dose	69	1.5	3.38 ± 0.01	
	Pulsed	3 frames/s	69	1.7	3.98 ± 0.01
		5 frames/s	69	2.9	6.46 ± 0.01
8 frames/s		69	4.3	9.53 ± 0.01	

cluded on Table 1 are approximately equivalent to the ones observed with the aluminum plates shown on Table 2. In some cases, the reduction in the entrance surface air kerma rate for the patient may achieve

67% according to the procedure to be performed.

The comparison between Tables 1 and 2 validates the method for determining the entrance surface air kerma rate by means of

a phantom adapted for fluoroscopy and demonstrates the equivalence between the phantom and the patient.

## CONCLUSIONS

The study of optimization of images in interventional fluoroscopy has demonstrated the relevance of a method for optimizing images quality and dose to the patients in this type of procedure.

The utilization of a phantom adapted for fluoroscopy allows the evaluation of the images quality besides determining the patient entrance surface air kerma rate.

The phantom allows the evaluation of the patient entrance surface air kerma rate as well as determining which exposure modes reduce the dose to the patient with no significant loss of diagnostic information. The evaluation of images obtained with the phantom, in cerebrovascular interventional procedures included, allows

the achievement of fluoroscopic images optimization.

## Acknowledgements

The authors thank Coordenação de Aperfeiçoamento de Pessoal de Nível Superior (Capes) for the financial support and the technical staff Hospital das Clínicas da Faculdade de Medicina de Ribeirão Preto da Universidade de São Paulo (HCFMRP-USP).

## REFERENCES

1. International Commission on Radiological Protection. Recommendations of the International Commission on Radiological Protection. ICRP Publication 26. Annals of the ICRP. 1977;1(3).
2. Brasil. Ministério da Saúde. Secretaria de Vigilância Sanitária. Diretrizes de proteção radiológica em radiodiagnóstico médico e odontológico. Portaria nº 453, de 1º de junho de 1998. Diário Oficial da União, Brasília, 2 de junho de 1998.
3. Secretaria de Estado da Saúde. Uso, posse e armazenamento de fonte de radiação ionizante no âmbito do Estado de São Paulo. Resolução SS-

625. Diário Oficial do Estado, São Paulo, 14 de dezembro de 1994.

4. Pina DR, Ghilardi Netto T, Rocha SL, et al. Construção de um fantoma homogêneo para padronização de imagens radiográficas. Radiol Bras. 2000;33:41-4.
5. Pina DR, Duarte SB, Ghilardi Netto T, et al. Optimization of standard patient radiographic images for chest, skull and pelvis exams in conventional x-ray equipment. Phys Med Biol. 2004;49: N215-26.
6. Parizoti A. Otimização de imagens e proteção radiológica em fluoroscopia [dissertação de mestrado]. Ribeirão Preto: Universidade de São Paulo; 2008.
7. Pina DR, Duarte SB, Ghilardi Netto T, et al. Phantom development for radiographic image optimization of chest, skull and pelvis examination for nonstandard patient. Appl Radiat Isot. 2009;67: 61-9.
8. Pina DR, Duarte SB, Morceli J, et al. Development of phantom for radiographic image optimization of standard patient in the lateral view of chest and skull examination. Appl Radiat Isot. 2006;64:1623-30.
9. Brasil. Ministério da Saúde. Secretaria de Vigilância Sanitária. Radiodiagnóstico médico: desempenho de equipamentos e segurança. Brasília: Ministério da Saúde; 2005.